Demonstration of tunable optical generation of higher-order modulation formats using nonlinearities and coherent frequency comb

Mohammad Reza Chitgarha,[1,*] Salman Khaleghi,[1] Morteza Ziyadi,[1] Ahmed Almaiman,[1] Amirhossein Mohajerin-Ariaei,[1] Ori Gerstel,[2] Loukas Paraschis,[2] Carsten Langrock,[3] Martin M. Fejer,[3] Joseph Touch,[4] and Alan E. Willner[1]

[1]*Department of Electrical Engineering, University of Southern California, Los Angeles, California 90089, USA*

[2]*Cisco Systems, Inc., 170 West Tasman Dr., San Jose, California 95134, USA*

[3]*Edward L. Ginzton Laboratory, Stanford University, Stanford, California 94305, USA*

[4]*Information Sciences Institute, University of Southern California, 4676 Admiralty Way, Marina del Rey, California 90292, USA*

**Corresponding author: chitgarh@usc.edu*

Received May 9, 2014; revised July 12, 2014; accepted July 15, 2014;
posted July 17, 2014 (Doc. ID 211820); published August 14, 2014

We demonstrate a tunable, optical generation scheme of higher-order modulation formats including pulse amplitude modulation (PAM) and quadrature amplitude modulation (QAM). Using this method, 100.4 Gbit/s 16-QAM and 120 Gbit/s 64-QAM were generated from 50.2 and 40 Gbit/s QPSK signals at EVMs of 7.8% and 6.4%, and 60 Gbit/s 8-PAM were generated at an EVM of 8.1% using three 20-Gbit/s BPSK signals. We also demonstrated a successful transmission of 80 Gbit/s 16-QAM through 80 km SMF-28 after compensating with 20 km DCF. All signals were generated, transmitted, and detected with BER below the forward error correction threshold.

OCIS codes: (060.2360) Fiber optics links and subsystems; (060.4370) Nonlinear optics, fibers; (190.4223) Nonlinear wave mixing.
http://dx.doi.org/10.1364/OL.39.004915

There has been significant interest in higher-order modulation formats for optical communication systems due to a combination of the need for increased data capacity and spectral efficiency in terms of bit/s/Hz [1,2]. With higher-order formats, the data are encoded at different levels of amplitude and/or phase with higher spectral efficiency. Such formats include: (a) quadrature phase shift keying (QPSK) as an example of 4-ary phase encoding; (b) 4 and 8 pulse amplitude modulation (4- and 8-PAM) as examples of 4- and 8-ary amplitude encoding; and (c) 16 quadrature amplitude modulation (16-QAM) as an example of 16-ary amplitude/phase encoding.

A conventional method for generating a higher-order data signal is to use the output from an electronic digital-to-analog converter to drive an in-phase/quadrature (I/Q) modulator [3–5]. However, key challenges for this approach are: (a) the limited linearity of the electronics at high baud rates, such that the spacing of the data constellation points on the I/Q plot will no longer be uniform and (b) electronic approaches may become difficult at rates exceeding 100 Gbaud [6].

As an alternative, nonlinear optical processes hold the promise of high-speed operation, format and phase transparency, low noise, and high linearity [7]. Examples of optical multiplexing in the phase and amplitude domains include: (i) a nonlinear-optical-loop-mirror can be used to optically multiplex four on–off-keyed (OOK) signals into one 16-QAM signal [8] and (ii) the multiplexing of two 20 Gbit/s QPSK signals into a single 40 Gbit/s 16-star-QAM [9]. However, these methods tended to be limited in terms of tunability. As an alternative approach, we recently demonstrated a method to multiplex three QPSK signals into a single 64-QAM signal using two cascaded, nonlinear stages, one stage to ensure coherency among the signals and the second stage to produce multiplexing [10]. However, two nonlinear stages tend to degrade the quality of the QAM signal that is generated. A laudable goal would be to use fewer nonlinear stages for better efficiency and lower power consumption.

We consider here the use of an optical frequency comb to remove the need for two nonlinear stages. Optical combs provide multiple wavelength "fingers" with very low linewidth, such that all the comb lines are coherent with each other [11]. This enables the ability to coherently manipulate the amplitude and phase of each individual finger and then efficiently process multiple fingers together [12].

In this Letter, we demonstrate tunable optical generation of higher-order modulation formats using nonlinearities and an optical frequency comb [13]. Due to the coherency of the comb fingers, coherent multiplexing can be accomplished in a single nonlinear stage resulting in better performance and lower power consumption. The comb lines are used as signal and pump sources. Using this tunable method, 100.4 Gbit/s 16-QAM, 80 Gbit/s 16-QAM, and 120 Gbit/s 64-QAM were generated from 40 and 50.2 Gbit/s QPSK signals at EVMs of 7.8%, 6.8%, and 6.4%, respectively. We used binary phase shift keying (BPSK) at 20 Gbit/s as the input signal to generate 40 Gbit/s 4-PAM, 40 Gbit/s QPSK, 60 Gbit/s 8-QAM, and 60 Gbit/s 8-PAM at EVMs of 8.1%, 8.3%, 8.5%, and 8.2%, respectively. Moreover, we demonstrated the transmission of 80 Gbit/s 16-QAM through 80 km of single mode fiber after compensating with 20 km of dispersion compensated fiber (DCF). All signals were generated, transmitted, and detected with BER below the forward error correction (FEC) threshold (3.8×10^{-3}).

Figure 1 shows the principle operation of our proposed optical higher-order signal generation scheme. First, a

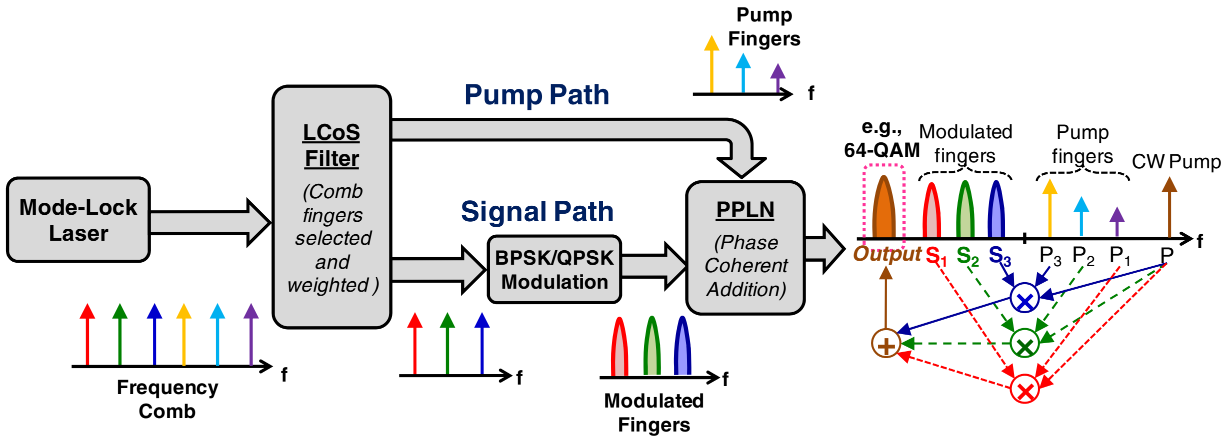

Fig. 1. Conceptual block diagram of a reconfigurable optical PAM/QAM generation scheme. In this configuration, the optical frequency comb fingers are separated into two paths, the signal path and the pump path. The signal path fingers are modulated to BPSK/QPSK signals and then injected into a PPLN waveguide after coupling with the pump fingers. In the PPLN waveguide, the modulated fingers, $S_i(t)$s, interact with the pump fingers $P_i(t)$s and the CW pump $P(t)$ to generate the output signals at higher-order formats.

mode-locked laser (MLL) generates multiple frequency comb fingers at different wavelengths. A liquid crystal on silicon (LCoS) programmable filter is used to select appropriate fingers and apply complex weights on the comb lines. Subsequently, an IQ modulator is used to modulate lower-order QAM signals on these comb fingers. Finally, these signals, along with another set of coherent comb fingers with equal frequency spacing and a CW pump laser, are injected into a nonlinear element to perform coherent addition. In our proposed scheme, only one periodically poled-lithium-niobate (PPLN) waveguide is used as the nonlinear stage for realizing multiplexing due to the coherency between the comb lines.

The MLL generates several tens of comb fingers that are located equidistantly in the frequency domain. The LCoS filter select two sets of the comb fingers at two separate signal and pump paths and apply amplitude and phase weights (complex coefficients c_is) on the comb lines in the pump path.

In the PPLN waveguide, each modulated comb line at ω_i and its corresponding nonmodulated line at ω_i' are located symmetrically around the PPLN's quasi-phase matching (QPM) wavelength ω_0 (i.e., $\omega_i' = 2\,\omega_0 - \omega_i$). Therefore, all signals $S_i(t)$ are mixed with the weighted pumps $c_iP_i(t)$ through independent sum-frequency-generation (SFG) nonlinear processes and generate $\sim c_iS_i(t)\cdot P_i(t)$ terms at $2\omega_0$. Because both the signals and the pumps are generated from coherent comb fingers, the generated terms are coherent with each other and thus coherently multiplexed [i.e., $\sim\Sigma c_iS_i(t)\cdot P_i(t)$].

A continuous wave (CW) pump at ω_P with an electric field $P(t)$ also is injected to the PPLN waveguide for the difference-frequency-generation (DFG) nonlinear process to convert the multiplexed signal to frequency $\omega_{\mathrm{Out}} \triangleq 2\omega_0 - \omega_P$. Hence, the electric field of the generated signal at ω_{Out} can be expressed as

$$S_{\mathrm{Out}}(t) = P^*(t) \times \sum_{i=1}^{N} c_iP_i(t).S_i(t), \qquad (1)$$

in which the complex coefficient c_i and the number of input signals (N) can be tuned to generate different signals. Therefore, the electrical data streams encoded on S_is create a higher-order signal (e.g., 16-QAM, 8-PAM, or 64-QAM) according to Eq. (1).

For BPSK signals, it is possible to generate PAM and QAM signals because the input signals can be combined in phase and/or in quadrature. Figure 2(a) shows the multiplexing of three BPSK signals to create an 8-PAM signal. As can be seen, the BPSK symbols are scaled by $c_1 = 1$, $c_2 = 0.5$, and $c_3 = 0.25$, respectively. A 4-QAM (QPSK) also can be generated from two BPSK signals when $c_1 = 1$ and $c_2 = j$ [Fig. 2(b)].

However, for the QPSK signal, because the data are encoded symmetrically on in-phase and quadrature phase in the complex plane, only the square QAM can be generated (i.e., 16-QAM, 64-QAM). Figure 2(c) shows that the weight set $c_1 = 1$, $c_2 = 0.5$, and $c_3 = 0.25$ for three QPSK signals can generate a 64-QAM signal.

Figure 3 shows the experimental setup of the proposed higher-order signal generation. An MLL with a 10 GHz

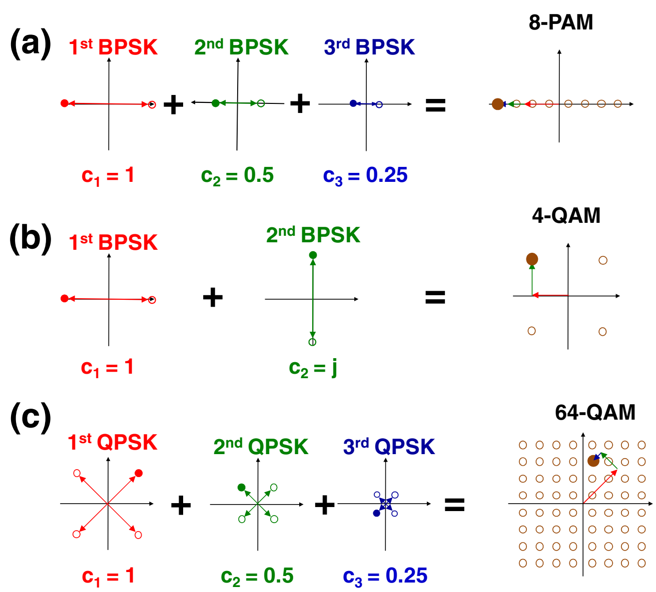

Fig. 2. Generating (a) 8-PAM, (b) 4-QAM (QPSK) signals using BPSK signals, and (c) 64-QAM using QPSK signals.

repetition rate and a 2 ps pulse width was used to generate a coherent comb with 10 GHz frequency spacing. This optical comb was sent to a delay-line interferometer (DLI) with a free spectral range (FSR) of 20-GHz for doubling the comb line spacing. Then, the 20 GHz comb was passed through a highly nonlinear fiber (HNLF) after sufficient amplification in an erbium-doped fiber amplifier (EDFA) to generate a flat and broadband spectrum. Figure 3 shows the optical spectra of (1) the optical frequency comb with 10 GHz frequency spacing at the MLL output, (2) the optical frequency comb with 20 GHz at the DLI output, and (3) the flat frequency comb at the HNLF output. Then, a liquid crystal on silicon (LCoS) filter was used to select and write complex weights on the comb fingers and separate them into signal path and pump path. Three comb fingers at wavelengths λ_{S1-3} of 1546.3, 1547.9, and 1549.5 nm were selected for the signal path, while another three comb lines at wavelengths λ_{P1-3} of 1550.5, 1552.1, and 1553.7 nm were assigned for the pump path. The comb lines at the signal path were sent into nested Mach–Zehnder modulators (MZMs) driven by 20 or 25.1 Gbit/s pseudorandom bit sequences (PRBSs) 231-1 to generate 20 Gbit/s BPSK or 40/50.2 Gbit/s QPSK signals (lower-order signals). Then, these signals were amplified, combined with the comb fingers at the pump path, and injected into 400 m DCF to induce one symbol delays between the signals. Then, an amplified CW pump laser at $\lambda_P =$ 1543.6 nm was coupled with the DCF output after enough amplification and sent to the PPLN waveguide with QPM wavelength $\lambda_0 = 1550$ nm for multiplexing. All modulated signal and comb lines were located symmetrically around ω_0 and interacted with each other through SFG nonlinear processes and created the multiplexed signal at $2\omega_0$ with appropriate complex coefficients. Then, the CW pump interacted with this multiplexed signal through the DFG nonlinear process and converted it to $\sim\lambda_{\mathrm{Out}} = 1556.6$ nm. It is worth noting that, in this demonstration, one modulator was used to encode the single data pattern for all input signals, and a DCF was used to induce delays between them. Therefore, this scheme performed higher-order modulation format generation with dependent data. However, for creating PAM and QAM data signals from independent data patterns it is required to encode the comb fingers in separate modulators, and then couple them together while maintaining the coherency between the signals [11].

Figure 4 shows the optical generation of higher-order modulation formats using multiple BPSK signals with different complex weights. The optical spectrum of the multiplexing stage at the PPLN output is shown for 40 Gbit/s QPSK and 60 Gbit/s 8-PAM signals in Figs. 4(a) and 4(b), respectively. For creating the QPSK signal, two 20 Gbit/s BPSK and two comb lines were required, whereas the 8-PAM signal can be generated by nonlinear interaction between three 20 Gbit/s BPSK and three comb fingers. Figures 4(c)–4(g) show data constellations for different higher-order modulation formats created from two or three 20-Gbit/s BPSK signals when they were weighted with complex coefficients and multiplexed coherently. Figure 4(c) shows two BPSK signals that are multiplexed with $c_1 = 1$ and $c_2 = 0.5$ to generate a 40 Gbit/s 4-PAM signal at an EVM of 8.1%. Figure 4(d) shows a 40 Gbit/s QPSK constellation with an EVM of 8.3%, which was generated by combining two BPSK signals of equal amplitudes and a 90° phase difference. Figure 4(e) shows three BPSK that are multiplexed coherently with coefficients $c_1 = 1$, $c_2 = 0.5$, and $c_3 = 0.25$ to generate a 60 Gbit/s 8-PAM signal with 8.2%. Figures 4(f) and 4(g)

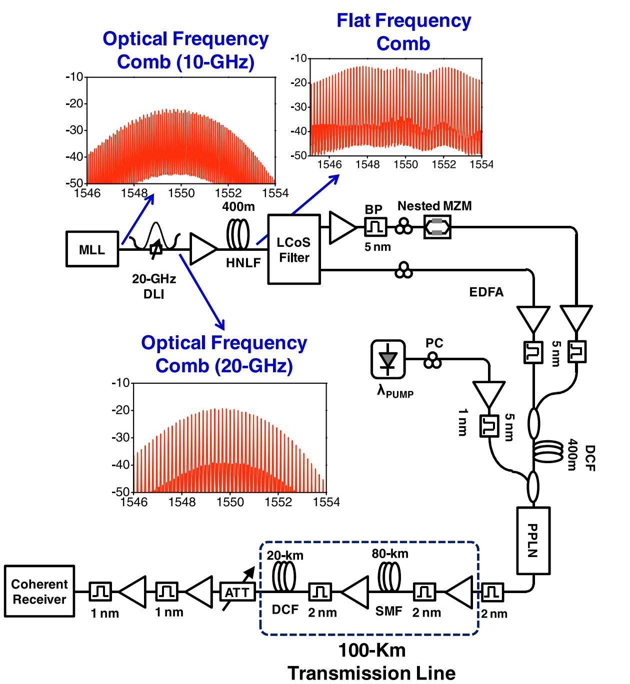

MLL: Mode-locked laser PC: Polarization controller
Nested MZM: Mach-Zender modulator DLI: Delay line interferometer
DCF: Dispersion compensating fiber BPF: Bandpass filter

Fig. 3. Experimental setup for the proposed optical QAM transmitter: a mode-locked laser is used to generate coherent frequency comb fingers.

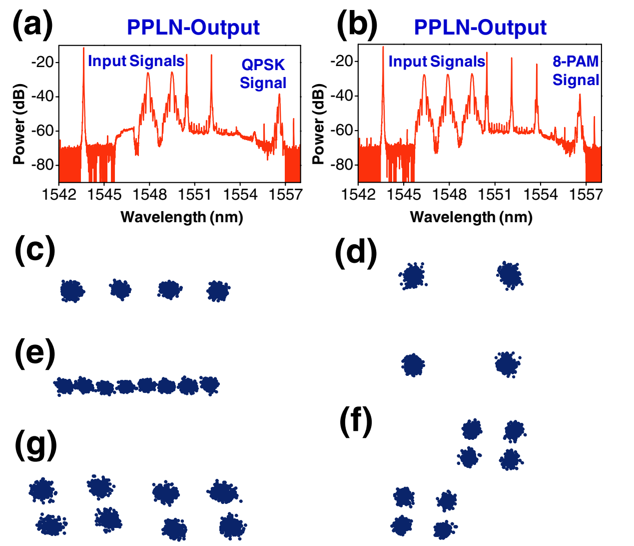

Fig. 4. Higher-level modulation format generation using BPSK signals. Optical spectrum of PPLN output when (a) a QPSK signal is generated using two BPSK signals and (b) an 8-PAM signal is generated using three BPSK signals. The constellation diagrams of (c) 40 Gbit/s 4-PAM, (d) 40 Gbit/s QPSK, (e) 60 Gbit/s 8-PAM, (f) 60 Gbit/s type-1 8-QAM, and (g) 60 Gbit/s type-2 8-QAM, with EVMs of 8.1%, 8.3%, 8.2%, 8.5%, and 8.7%, respectively.

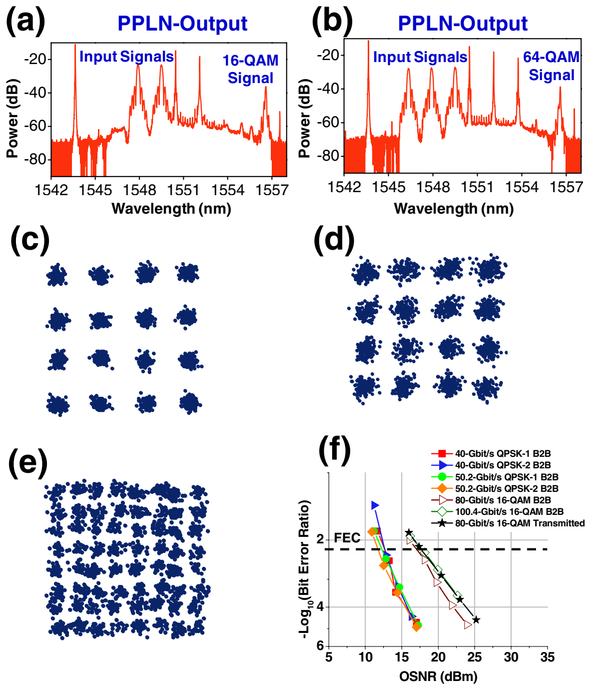

Fig. 5. Square QAM generation using QPSK signals: optical spectrum of PPLN output when (a) a 16-QAM data signal was generated using two 40 Gbit/s QPSK signals and (b) a 64-QAM data signal was generated using three 40 Gbit/s QPSK signals. The constellation diagrams of (c) 80 Gbit/s 16-QAM, (d) 100.4 Gbit/s 16-QAM, and (e) 120 Gbit/s 64-QAM, with EVMs of 6.8%, 7.8%, and 6.4%, respectively. (f) BER assessments of the back-to-back (B2B) QPSK signals, generated 80 Gbit/s and 100.4 Gbit/s 16-QAM signals, and the transmitted 80 Gbit/s 16-QAM signal.

show two types of 60 Gbit/s 8-QAM constellations with EVMs of 8.5% and 8.7% that were generated from three BPSK signals with $c_1 = 1$, $c_2 = 0.5$, and $c_3 = 0.5j$ and $c_1 = 1 + j$, $c_2 = 0.5$, and $c_3 = 0.5j$, respectively.

Figure 5 shows the combination of two or three 40 Gbit/s or 50.2 Gbit/s QPSK signals to create higher-order QAMs. The spectrum of the PPLN output is depicted for 80 Gbit/s 16-QAM and 120 Gbit/s 64-QAM signals in Figs. 4(a) and 4(b), respectively. In the 16-QAM case, two modulated and two unmodulated comb fingers were used whereas for the 64-QAM signal, three QPSK and three comb lines were involved. Figure 5(c) shows the 16-QAM constellation with an EVM of 6.8% at 80 Gbit/s when complex coefficients $c_1 = 1$, $c_2 = 0.5$ were applied on two 40 Gbit/s QPSK signals. The same complex weights were used to generate 100.4 Gbit/s 16-QAM with an EVM of 7.8% from two 50.2 Gbit/s QPSK signals in Fig. 5(d). In order to generate a 120 Gbit/s 64-QAM signal with an EVM of 6.4%, the complex coefficients $c_1 = 1$ and $c_2 = 0.5$ were applied on three 40 Gbit/s QPSK signals [Fig 5(e)]. The quality of the generated 64-QAM is lower than the other constellation which we believe was a result of significant noise from S_3 because it was attenuated 12 dB.

The BER estimations were assessed to evaluate the performance of the generated signals in Fig. 5(f). This BER measurement is directly performed in the coherent receiver. The BER versus the received optical signal-to-noise ratio (OSNR) curves for input QPSK signals at 40 and 50.2 Gbit/s are shown for reference. The generated 80 and 100.4 Gbit/s 16-QAM for the back-to-back is shown. The generated 100.4 Gbit/s 16-QAM showed slight degradation in the BER assessment, which we believe was due to the effect of the lower conversion efficiency at the higher baud rate that can be due to the quasi-phase matching condition in the PPLN waveguide. It was shown that the 80 Gbit/s 16-QAM signal could be transmitted through a 100 km fiber link (80 km SMF-28 and 20 km DCF) under FEC threshold.

This work was made possible by support from NSF, CIAN, DARPA, and Cisco Systems.

References

1. G. Li, Adv. Opt. Photon. **1**, 279 (2009).
2. A. H. Gnauck, P. J. Winzer, A. Konczykowska, F. Jorge, J.-Y. Dupuy, M. Riet, G. Charlet, B. Zhu, and D. W. Peckham, J. Lightwave Technol. **30**, 532 (2012).
3. Y. Koizumi, K. Toyoda, M. Yoshida, and M. Nakazawa, Opt. Express **20**, 12508 (2012).
4. A. Sano, T. Kobayashi, K. Ishihara, H. Masuda, S. Yamamoto, K. Mori, E. Yamazaki, E. Yoshida, Y. Miyamoto, T. Yamada, and H. Yamazaki, *European Conference on Optical Communication (ECOC)* (2010), paper PD2.4.
5. R. Schmogrow, D. Hillerkuss, M. Dreschmann, M. Huebner, M. Winter, J. Meyer, B. Nebendahl, C. Koos, J. Becker, W. Freude, and J. Leuthold, IEEE Photon. Technol. Lett. **22**, 1601 (2010).
6. G.-W. Lu, T. Sakamoto, and T. Kawanishi, Opt. Express **21**, 6213 (2013).
7. G. Agrawal, *Nonlinear Fiber Optics* (Academic, 2001).
8. G. Huang, Y. Miyoshi, A. Maruta, Y. Yoshida, and K.-I. Kitayama, J. Lightwave Technol. **30**, 1342 (2012).
9. X. Wu, J. Wang, H. Huang, and A. E. Willner, *Conference on Lasers and Electro-Optics* (2011), paper CThH4.
10. M. R. Chitgarha, S. Khaleghi, Z. Bakhtiari, M. Ziyadi, O. Gerstel, L. Paraschis, C. Langrock, M. M. Fejer, and A. E. Willner, Opt. Lett. **38**, 3350 (2013).
11. J. Pfeifle, V. Brasch, M. Lauermann, Y. Yu, D. Wegner, T. Herr, K. Hartinger, P. Schindler, J. Li, D. Hillerkuss, R. Schmogrow, C. Weimann, R. Holzwarth, W. Freude, J. Leuthold, T. J. Kippenberg, and C. Koos, Nat. Photonics **8**, 375 (2014).
12. M. Ziyadi, M. R. Chitgarha, S. Khaleghi, A. Mohajerin-Ariae, A. Almaiman, J. Touch, M. Tur, C. Langrock, M. M. Fejer, and A. E. Willner, Opt. Express **22**, 84 (2014).
13. M. R. Chitgarha, M. Ziyadi, S. Khaleghi, A. Almaiman, A. Mohajerin-Ariaei, L. Paraschis, O. Gerstel, C. Langrock, M. Fejer, J. Touch, and A. E. Willner, *Conference on Lasers and Electro-Optics (CLEO)* (Optical Society of America, 2013), paper CTu1G.2.